Short-time evolution in the adaptive immune system

Nicholas Guttenberg, S. M. Ali Tabei, and Aaron R. Dinner

Phys. Rev. E **84**, 031932 — Published 30 September 2011

DOI: 10.1103/PhysRevE.84.031932

Short-time evolution in the adaptive immune system

Nicholas Guttenberg, S. M. Ali Tabei, Aaron R. Dinner
James Franck Institute, The University of Chicago, Chicago, IL 60637

We exploit a simple model to numerically and analytically investigate the effect of enforcing a time constraint for achieving a system-wide goal during an evolutionary dynamics. This situation is relevant to finding antibody specificities in the adaptive immune response as well as to artificial situations in which an evolutionary dynamics is used to generate a desired capability in a limited number of generations. When the likelihood of finding the target phenotype is low, we find that the optimal mutation rate can exceed the error threshold, in contrast to conventional evolutionary dynamics. We also show how a logarithmic correction to the usual inverse scaling of population size with mutation rate arises. Implications for natural and artificial evolutionary situations are discussed.

PACS numbers: 87.23.Kg, 87.19.xw

I. INTRODUCTION

Normally in population genetics, a novel mutation becomes ubiquitous in a population before new mutations occur at the same locus—this is the process of fixation. This reflects the time scale of the development of new phenotypes, which is usually very long due to the fact that the mutation rate is small compared to the rate at which the new mutation expands in the population. There are examples of systems where the mutation rate is large, leading to evolutionary dynamics without fixation.

Quasispecies theory is used to model these systems[1–3]. Furthermore, systems are often exposed to short-timescale fluctuations due to changing environments, which can change the evolutionary dynamics [4]. We investigate the case where the effect of the short-timescale influence is absolute. That is, rather than a system exposed to a time-varying stress (to which the system may respond in many different ways), we ask what happens when an evolution has a fixed time limit, after which the population as a whole is considered to have failed.

This situation is seen in the adaptive immune system. During the immune response, discovery of new antibody specificities (phenotypes) and the dominance of high affinity clones (fixation) occur on similar time scales of tens of generations by way of somatic hypermutation [5, 6]. Failure to discover responding antibodies within a certain time interval can lead to the death of the host.

Another example where this applies is in artificial genetic algorithms. Directed evolution is used for industrial applications: protein design[7], optimized wing aerodynamics[8], the design of support structures[9, 10], and many other systems. In such applications, the evolutionary timescale is compressed as much as possible towards the goal of developing a specific functionality, in which case beneficial mutations may not have time to become fixed. Similarly, in artificial systems such as applied genetic algorithms, it is desirable to make the simulation converge upon a good solution as quickly as possible, and as such one can utilize any evolutionary parameters that yield at least one optimal instance, even if the population of its descendents would be unstable under continued mutation.

In all of these cases, only a single successful individual must be discovered by the end of the adaptive phase of the process, and it can then be amplified after reduction of the mutation factor (as in the immune system) or by the experimenter extracting and analyzing the successful case. This objective contrasts with that for competing organisms, in which population stability is often more important than the discovery of rare beneficial mutations. We thus expect the optimal evolutionary dynamic to maximize the system-wide fitness rather than be tuned for the expansion of individuals and their descendents. This represents a form of altruism [11], in that individual members sacrifice their own expansion, e.g., by having harmfully high mutation rates, to help achieve the system-wide goal. In the present study, we develop a model to explore these evolutionary dynamics and understand how best phenotypes can be generated in short times.

To ground our model in reality, we cast it in terms of the adaptive immune system. The humoral immune response centers on activated production of antibodies by B lymphocytes, each with some affinity to the antigen. The initial generation of activated B cells comes from a pool of naive cells (or clones), each with particular rearrangements of the heavy- and light-chain variable regions that determine the antibody specificity. B cells with antibodies with high affinity for the antigen are most strongly activated, and undergo an increase in both their replication rate and their mutation rate. This leads to an evolutionary dynamic in which higher affinity subpopulations of B cells grow more rapidly (as they more frequently bind to antigen) and eventually dominate the system. The increased mutation rate (compared to resting B cells) also allows for novel sequences to be discovered, leading to a form of evolution in which new B-cell specificities are developed on the same time scale as their population dynamics.

Evolutionary aspects of the adaptive immune system have been extensively modeled in prior work. Abstract models of affinity maturation have been used to gauge

the rate of response to antigens [12]. These models have accurately predicted qualitative details of the immune response, and have hinted at the importance of secondary mechanisms for achieving quantitative agreement with experimental observations [13, 14]. Furthermore, this sort of modeling has been used to understand how the process of adaptation leads to the generation of memory, and how hyperspecificity can lead to a poor secondary response (original antigenic sin) [15, 16]. Our focus is less on a quantitative replication of the course of a particular infection as it is to understand what generic changes to the evolutionary dynamics can emerge due to the short time scales and high mutation rates.

To this end, we exploit a simple representation of B-cell specificity to model the evolutionary dynamics of the primary immune response. Given that we consider evolutionary pressure to be on the host, rather than directly on the components of the adaptive immune system, we expect that we can capture the observed B-cell hypermutation rate by optimizing the system-wide success rate. We model the host-scale success or failure by considering a time limit on the evolutionary dynamics (T), at which point the system has succeeded at maturation to a particular antigen to a certain degree, and this defines a system-wide fitness.

We use the simulations to estimate the dependence of the probability of success on the mutation rate, and then we show that these curves can be described analytically in terms of a uniform volumetric search. In this picture, the scale of the search volume is determined by mutation rate and time. The unique sequences that are produced by the dynamics randomly cover this search space, and we evaluate the probability that at least one of those sequences lies within the target region. To predict the success rate using this picture we need to know the total number of unique sequences produced by the end of the evolutionary interval. To this end, we compute the dependence of the final population size on the mutation rate and, in turn, the theoretical success rate curves. Remarkably, despite the strong selection that we impose on antibody affinity in the simulations (which would suggest that the actual set of search paths should be highly relevant), the volumetric search picture successfully captures the salient aspects of the dependence of the success rate on mutation rate and time limit T.

From the simulations, we also compute the optimal mutation rate. In conventional evolutionary dynamics the mutation rate is normally limited by the error threshold [17, 18]: $\mu \leq \log(\sigma)/L$, where σ is the selection strength and L is the genome length. In the case where one is considering the distinction between a fitness peak and a survivable plateau (that is, the plateau corresponds to a state with no lethal mutations), this threshold determines the point at which selection fails to maintain information about the peak. When distinguishing between a peak and a lethal valley, the threshold no longer applies [1], as any offspring generated in the lethal valley simply die, and so the population does not forget the peak, but does risk extinction. If one is attempting to find higher fitness peaks from within a fitness valley, the error threshold does apply, and normally limits the optimal mutation rate of the system.

The error threshold is the mutation rate over long times at which a system loses the ability to maintain a fitness maximum. If the system has a time-variable mutation rate[19] (that is, it shuts down mutation after T has been reached and then allows the system to grow) then the error threshold of the high-mutation period need not actually constrain the optimal mutation rate in all cases. Basically, a short-duration spike of the mutation rate followed by a period of low mutation can have an average rate of mutation below the error threshold, even though instantaneously the mutation rate crosses the error thresold.

However, if a large portion of the population dies due to failed mutations, then fewer sequences can be explored during the time available. It is the interplay between these two effects that constrains the evolutionary dynamics. We find that the instantaneous optimal rate can be above the error threshold, but only in those cases where there is a low chance of success overall. Implications of the results for the immune system and artificial evolutionary situations are discussed.

Methods

We use a string-based model of antibody-epitope affinity (similar to [20] and others) to understand the consequences of fast macroevolution. In such models, each molecule (antibody or epitope) is represented by a sequence of values. Matching values at corresponding points in the antibody sequence and the epitope sequence increase affinity, while unlike pairs decrease affinity. In these models, the affinity is then some function of the Hamming distance between the two sequences: the total number of matches. Here, we use a base-4 representation.

Our simulations consist of a set of B cells, each of which produces a specific antibody. They evolve via selection on the initial population and by mutation to maximize affinity with one of a number of target epitopes N_e of the invading virus. The target epitopes and the antibodies produced by the B cells are both represented by a string of bases of length L. The affinity between an antibody and a set of epitopes is the maximum of the affinity A between the antibody and each of the epitopes present; it is defined to be the number of matches between the antibody string (x^k) and the epitope string (y^i):

$$A_k = \max_i d_i \tag{1}$$

where

$$d_i \equiv \sum_j \delta_{x_j^k, y_j^i} \tag{2}$$

is the Hamming distance between antibody and epitope, and δ is the Kronecker delta.

This representation gives rise to an additive fitness function. Recently, there has been interest in multiplicative fitness landscapes[21, 22]. These are fitness landscapes in which the factors given by each feature of the organism to control its replicative success rate are multiplied rather than added. This has the consequence that the dominant factor to replication rate of the organism is its worst feature, and so the evolutionary process emphasizes removing negative aspects before developing new positive aspects. One consequence of this type of landscape is that specific mutations can give rise to lethality regardless of whether an individual has other, positive traits. This could be relevant to the immune system in that mutations that dramatically decreased the surface expression of the receptor regardless of its affinity for antigen could lead to death of a clone. As discussed below, the growth rate depends exponentially on the affinity, and we work primarily in the infinite selection strength limit. In this limit, the difference in replication rate between the most fit clonal line and the second most fit clonal line becomes exponentially large, in effect killing (or at least neutralizing) all mutations that do not at least maintain the current fitness. Therefore we expect that in this limit there is no strong dependence on the overall structure of the fitness landscape (multiplicative or additive), as all mutations will either create a new high-fitness cell line, do nothing, or neutralize the B-cell with respect to replication.

The landscape that we use does not have interdependence between bases—it is a fairly easy problem. More convoluted landscapes occur biologically, in which there is epistasis and more general co-dependence between mutations. For much of this work we consider the infinite selection strength limit, in which epistasis insufficient to create a fitness barrier is equivalent to the case of no epistasis. In general however, there can be situations where gene interactions make it necessary to go uphill first in order to find the global optimum. These may include "glassy" problems in which frustration is possible, requiring large-scale sequence changes in order to escape a local optimum [4]. In our case, our model concerns the approach to a local minimum of the immune space, as the large population of naive B-cells provides redundancy in the form of covering the immune space. As such, we expect the naive B-cells to be initialized in the basins of attraction of the target minima.

A cell with affinity A_k establishes a population that grows as $(1+r_k)^t$ (where t here is the generation number, not the physical time) where the replication rate of this set of cells is

$$r_k = C\exp(\gamma A_k), \tag{3}$$

C is a population-wide normalizing factor and γ indicates the strength of selection. C is chosen so that the total replication rate of the fastest growing B-cell in the population is 2 to create a non-dimensionalized time scale in terms of the number of cell doublings. As a consequence of this rescaling of the growth rate, the absolute time allotted for evolution is not fixed. Our choice is reasonable in systems where the resources needed for replication are limited. In that case, if one organism is much more fit than the others, the result will be that it will still have some fixed replication rate corresponding to resource saturation. Here, the limiting factor is the availability of activation factors. B-cells that identify the antigen present it to helper T-cells, which activate the B-cell increasing its replication rate. In a B-cell population with varying specificities to the antigen, there is competition between B-cells for the antigen and for the helper T-cells, both of which could potentially limit the B-cell replication rate. The normalization of the growth rate leads to an effective interaction between otherwise independently growing cell lines. This can lead to a form of clonal interference. If two different mutations are discovered by the system in different cell lines, then only one of those mutations is likely to be further explored, specifically whichever gains a second beneficial mutation first. Once that happens, the other mutation, even if useful, will be frozen out. In effect, two simultaneous but different beneficial mutations will interfere with each other as they are competing for dominance within the population.

When a cell replicates in this model, each base of its string mutates with probability m/L, so that the global mutation rate is m. With regard to the selection strength, we observe little change in the numerical results when $\gamma > 1$ (see inset of Fig. 2), so we only consider the limiting behavior for strong ($\gamma \gg 1$) and weak ($\gamma \approx 0$) selection. While clones of varying affinities will clearly contribute to an actual immune response, we exploit the insensitivity to the value of γ in deriving our analytical results and work in the infinite selection strength limit ($\gamma \to \infty$) as it is more tractable than the finite selection strength case. We can estimate a biologically reasonable value of γ using the results of [23], in which an amplification factor of 125 in 10 generations was reported (corresponding to 15625 in 20 generations). Using the inset of Fig. 2, this corresponds to approximately $\gamma = 0.7$, which is at the border of the strong selection and weak selection limits.

We also make the choice to consider only relative cell growth factors, rather than the influence of cell death. During a primary immune response, cell replication rates are enhanced above the normal level. While cell death does occur, much of its evolutionary effect can be expressed in a modification of the growth rate of the different cell populations. As such, we expect to observe a series of exponentially growing subpopulations of B-cells. We also assume that the population can continue to grow exponentially without limit for the duration of the response. Because of this, we can take the entire immune response consisting of the responses to many epitopes across many germinal centers and consider the characteristic dynamics of the response of a single cell line to a single epitope. Within the context of our model, these populations would only interact by competing for activation, but this would not happen strongly between

germinal centers, and so we can consider the dynamics of a single germinal center's subpopulation that reacts to a single epitope independently from the others. Each separate epitope and each separate germinal center are additional chances to produce immunity. We may then compute the combined probability of finding a successful sequence across the whole set of initial conditions. If the probability of success for evolution around a single epitope is p, then the probability of success for evolution around any of N_e epitopes is $1-(1-p)^{N_e}$.

We define success here as whether or not a sequence with sufficient affinity is discovered after a fixed amount of time, where the threshold for sufficient affinity can be varied as a model parameter. One could argue that average affinity is a better indicator of the strength of response to the infection, but once a high affinity cell has been discovered it will be strongly activated and clonal amplification will take place. There is no need to actually simulate this process as it is simply a growth curve with the growth rate of that high affinity clone. To correct for this, we take into account how long it would take for clonal amplification to expand a single cell into a reasonable germinal center B-cell population of around 1000 cells[23]. This means that the time intervals over which we explicitly simulate are shorter than the total duration of the immune response, and the T values considered reflect this.

We initialize the system with a single cell at an initial Hamming distance d_0 from one of the epitope sequences. We then let it evolve for T generations and check if at least one cell with distance $d_t < d_0$ is present in the system. If such a cell is found, then the system is considered to have succeeded at adapting to the invader. If such a cell is not found, then the system has failed to combat the infection. We repeat this experiment and average over 1000 trials to determine the average success rate. We vary T, d_0, and $D = d_0 - d_t$ to gauge the ability of the immune system to make some number of beneficial mutations in the period of hypermutation as a function of these parameters.

The parameters of the model L and T need to be chosen realistically for the immune system, as the results depend very strongly on both. A B cell has a variable region in its genome of about 660 bases due to VDJ recombination, and within this variable region are hypervariable complementarity determining regions (CDRs) that determine specificity, comprising between 20% and 30% of the variable region [24]. Furthermore, mutation is not evenly distributed across the hypervariable regions. Certain motifs (RGYW/WRCY) tend to concentrate mutations [25] and lead to a reduction in the effective length of the dynamic component of the genome by a factor of up to 3/32 for a random sequence. Experimentally, half of the mutations that occur during hypermutation are associated with RGYW/WRCY motifs and there is strong codon bias favoring G and C mutations [26]. As such the relevant length of our antibody strings is some where between $L = 12$ at minimum to $L = 200$ at maximum (assuming every site in the hypervariable region has a uniformly high mutation rate). We investigate $L = 30$ and $L = 150$ as representative relevant lengths.

A generalized timeline of infection suggests that the time from infection to the peak of the primary non-specific immune response is from 3 to 14 days [27]. During this time, adaptive immunity must select for higher affinity B cells to become memory cells that participate in the secondary immune response. Activated B cells have a wide variation in division rates related to the mechanism of isotype switching, with the fastest dividing cells in the system dividing approximately twice a day [28]. As such, the adaptive immune system must develop a broad repertoire of mutated B cells during the initial period of from 6 to 28 generations, which may then be amplified to the point of clonal dominance during the remaining time that the infection is resident in the body. We investigate adaptation durations of $T = 10$, $T = 15$, $T = 20$, and $T = 25$ generations. A single run of this model is shown in Fig. 1a and b.

II. RESULTS

In this section, we use our model to illustrate how fast macroevolution of the adaptive immune system differs from standard evolutionary dynamics. If we consider the final population size in the limit of infinite selection, in general we expect an inverse dependence on the mutation rate as organisms develop harmful mutations. In both fast macroevolution and standard dynamics, this corresponds to the fraction of offspring who are non-viable due to harmful mutation. However, due to the rapid discovery of beneficial mutations we expect that this inverse dependence should be tempered in the case of fast macroevolution. We predict the correction factor and compare with numerical experiments. We also predict how the success rate of adaptation toward a given target should scale with mutation rate, allowing us to determine the optimum mutation rate.

A. Fixation time

In the usual picture of evolutionary dynamics, there is a separation between the time to develop new mutations and the time for mutations that are introduced to become present in every member of the system or to become extinct (fixation time). We first verify that the adaptive immune system is operating in a regime in which the development of beneficial mutations and the process of fixation have similar time scales. To this end, let us consider the introduction of a high affinity clone into a population P_0 comprised of clones with a baseline level of affinity. We would like to compare the fixation time of this new clone with the rate of introduction of beneficial mutations. Fixation is based upon the extinction of either the new line or the old line of cells, which is

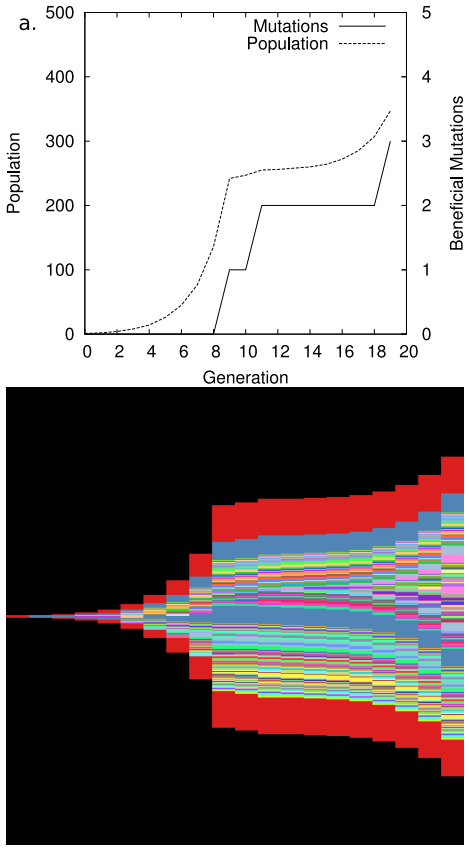

FIG. 1: (a) Data from a single run of the simulation with $L = 30$, $\gamma = \infty$, $T = 20$, and $d_0 = 10$. The total cell population is shown, along with the number of beneficial mutations discovered at that point in time. Every time a new beneficial mutation is discovered, that sub-population must expand, leading to a series of sequential exponential growths in the population. (b) (Color online) Muller plot of the same simulation. The outline of the plot shows the growth of the population, and the separate colors are different mutated cell lines plotted in the center of their parent cell line.

limited by the mortality rate. However, the time scale of the immune response is such that the mortality rate of B cells that are not of the high-affinity cell line will be much slower than the actual dynamics of interest. As such, rather than the time to fixation, we consider the time for the high-affinity clone to become the dominant contributor to the response (clonal dominance [29]); we take this time to be that at which the newly introduced clone has a population equal to the rest of the B cell pool.

Let us consider affinity-driven selection on the growth rate. We can do this either by assuming a growth rate that increases with affinity, or by assuming that there is some background death rate that is decreased by high affinity. In either event, we can discuss both of these scenarios in terms of the doubling time of the (surviving) population. We will mark time by the progress of the highest affinity population for ease of computation: we define the doubling time of the highest affinity population to be one generation. In reality, the rate of growth of the highest affinity population may change in time, and so to determine an exact mapping between generation number and physical time one needs to know exactly how the net growth rate depends on affinity. We perform all of our calculations in this generation time scheme so that we can determine what results are independent of the choice of model for the connection between affinity and growth rate. With such a model (e.g., [30]), all of our generation-based times can in principle be converted to physical times. In cases where we need to reference physical times, such as in the overall duration of our process, we use the average growth rate of the entire germinal center B-cell population to convert timescales as a first approximation.

In this notation, the high- and low-affinity populations expand in time as $P_h(t) = 2^t$ and $P_l(t) = P_0(1 + r_2)^t$ with $(0 < r_2 < 1)$, respectively, so that $P_h(t) = P_l(t)$ at $t = \log(P_0)/[\log(2) - \log(1 + r_2)]$. If the new B-cell population is doubling every generation with respect to a fixed baseline population (corresponding to $r_2 = 0$), then it takes a new subpopulation as long to overtake the existing population as it took to establish the original one. As such, the maximum timescale for fixation is of the order of the timescale of the immune response—around 20 or 30 generations. This corresponds to the maximum number of cells that could be produced from a single initial B-cell over the course of the immune response. It has been observed that actual clonal dominance occurs somewhat faster than this in the immune system[31], suggesting that in the case of the immune response the baseline population is not holding constant but is actually decreasing. This difference is consistent with our choice to approximate the underlying death rate of cells as a modification to the replication rate.

We can compare this to the timescale for the discovery of beneficial mutations. Given that the rate of hypermutation in the immune system is approximately 10^{-3} per basepair, corresponding to one mutation every two generations [32], let us consider the slowest scenario for the discovery of a beneficial mutation. For a long characteristic sequence length $L = 200$ in which there is only a single specific possible beneficial mutation to be found, we would need a population of 1200 descendents uniformly covering the space of possible mutations to have an $O(1)$ probability of having found that mutation. This corresponds to a time scale of 17 generations starting from only a single cell (and fewer with an existing growing population), which is comparable to the fixation timescale.

B. Population

The final population of B cells constrains how many sequences can be explored in total during the period of affinity maturation. In the limit of zero selection strength, the final population of B cells would be 2^T, where T is the number of generations. In the infinite selection strength limit, however, only the current best

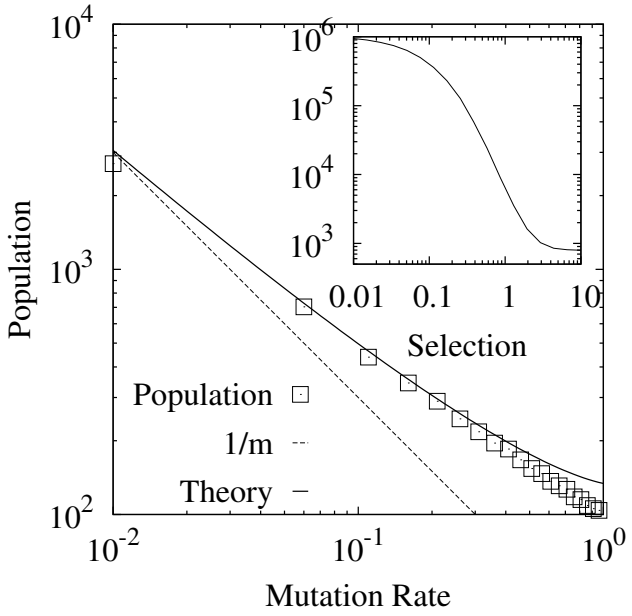

FIG. 2: Population dependence on the mutation rate. We plot the total population at the end of the interval of evolution. The solid line is our theoretical result (Eq. 10) with no free parameters. $L = 30$, $\gamma = \infty$, $T = 20$, and $d_0 = 10$. The inset shows the dependence of the results on selection strength γ for $m = 0.05$. For values of $\gamma \gg 1$, the resultant population approaches the infinite selection strength asymptotic limit.

subpopulation grows at all; the total population then becomes a sum of a set of subpopulations, each of which grew while that specificity was the best but stopped growing upon the emergence of a new beneficial mutation.

Fig. 2 shows the final population as a function of mutation rate, m, for a system at time $T = 20$, starting from an initial distance in sequence space of $d_0 = 10$, and in the infinite selection strength limit, $\gamma = \infty$. Power-law behavior is observed for small m, and the final population decreases monotonically as m increases. Conceptually this makes sense—as m increases, so too do the number of harmful mutations that occur during the growth of the system, thus reducing the expanding component of the population. Furthermore, as the rate of discovery of beneficial mutations increases, large parts of the system are left behind and do not grow as quickly. out any free parameters Let us now see how we can understand the population scaling that we see in our simulations. For a subpopulation that has already obtained n beneficial mutations, the probability of a single mutation improving the affinity, p_+, is the product of the fraction of sites remaining with mismatches $(d_0 - n)/L$ and the fraction of alternative values that would result in a match for each such site (1/3 for our base-4 representation). Because the subpopulation continues to grow so long as no beneficial mutations occur, we must compute the average time τ between beneficial mutations to obtain the total population growth. The cumulative probability that a beneficial mutation is found by time t is

$$p = 1 - (1 - p_+)^{m2^t} \tag{4}$$

where $m2^t$ is the total number of mutations made by the subpopulation, neglecting corrections to the growth owing to deleterious mutations.

We proceed by assuming that the rate of beneficial mutations per individual cell division, $r_+ \equiv mp_+$, is small (by definition, $r_+ \leq 1/3$). This is reasonable for both difficult evolutionary problems (close to the optimum) and small mutation rates. We can thus expand p to obtain $p \approx r_+ 2^t$. The probability of having found a beneficial mutation approaches 1 when $t = \tau$ for

$$\tau(n) = -\log_2 r_+ = \log_2 3L/m(d_0 - n). \tag{5}$$

We now want to obtain the (average) final number of beneficial mutations, n_f, in total evolution time T, regardless of whether the search was successful ($n_f = d_0$) or not ($n_f < d_0$). Approximating n as a continuous variable,

$$T = \int_0^{n_f} \tau(n) dn. \tag{6}$$

We consider two limiting cases. If the optimum sequence is easily found ($n_f/d_0 \approx 1$) then we expect to quickly obtain a single exponentially growing population. In this limit we recover the general case of $P \approx m^{-1}$. On the other hand, for hard evolutionary problems, we are sufficiently far from the optimum that we do not consistently find it, and so $n_f/d_0 \ll 1$. We now discuss the latter case in depth.

Substituting Eq. 5 into Eq. 6, integrating, expanding the resulting logarithms, and keeping terms to second order in n_f/d_0, we obtain

$$n_f^2 + 2d_0 n_f Q(m) - 2d_0 T \log(2) = 0, \tag{7}$$

where $Q(m) \equiv \log(3L/md_0)$. Solving for n_f,

$$n_f = -d_0 Q \left(1 - \sqrt{1 + \frac{2T}{d_0 Q^2}}\right). \tag{8}$$

Employing Eqs. 5 and 8, the final population of cells is

$$P = \int_0^{n_f} 2^{\tau(n)} dn \tag{9}$$

$$= -\frac{3L}{m} \log\left[1 + Q\left(1 - \sqrt{1 + \frac{2T}{d_0 Q^2}}\right)\right]. \tag{10}$$

Keeping in mind the dependence of Q on m, we see that, to first order in $1/\log m$,

$$P \sim m^{-(1+1/\log m)}. \tag{11}$$

In Fig. 2 we plot the prediction of Eq. 10 (solid line) against the results of our simulation. The predicted curve fits the data well with no free parameters. For comparison, the leading order $1/m$ behavior is also shown (dashed line). The effect of the logarithmic corrections in the relevant range of mutation rates is sufficient to change the apparent scaling exponent by about 25%.

The difference from the standard picture that has given rise to this logarithmic correction is that because the evolutionary timescale is faster than the timescale of cell death in this system, old cell populations still remain in the system even after they have been made obsolete by the discovery of beneficial mutations. As such, rather than having one dominant species that contributes to the population, the resultant population contains a memory of the evolutionary trajectory leading to the current state in the residual subpopulations.

Now that we have a theory for the final population of sequences, we can estimate how many different sequences are explored by the system. Using this, we can then understand how the rate of success of the fast macroevolutionary process depends on mutation rate.

C. Success Rate

We now consider the likelihood that the immune system will find a sufficiently high-affinity receptor to have a response. Beyond a certain required distance of adaptation, the system will often fail, but the presence of multiple B cell lines independently evolving can greatly amplify the chance of success. With this in mind, we examine the dependence of the success rate on the system parameters for a cutoff in the individual success rate of 10%. Below this point, the success rate decays very quickly and becomes difficult to measure accurately in our simulations. Note that the success rate we measure concerns adaptation to a single epitope. If multiple epitopes are available, each epitope will attract a population of B cells. As such, each epitope can be viewed as an independent trial. For N_e epitopes and an individual probability of success S, the overall success rate is $1-(1-S)^{N_e}$. This means that an individual 10% success rate corresponds to a 65% system-wide success rate if there are ten epitopes, an 88% success rate if there are twenty epitopes, and so on.

In Fig. 3, we plot the success rate as a function of mutation rate for different success thresholds, D, in the infinite selection limit ($\gamma = \infty$). These data tell us the ability of the system to respond to an epitope, as well as the mutation rate that optimizes the chance of success. We would like to construct a picture that allows us to understand and predict these curves. To do this we construct a simple approximation in which there is a search space of sequences constructed by the set of mutations, and all sequences explored by the system are randomly chosen from this search space. This is somewhat analogous to the shape-space approaches used to understand

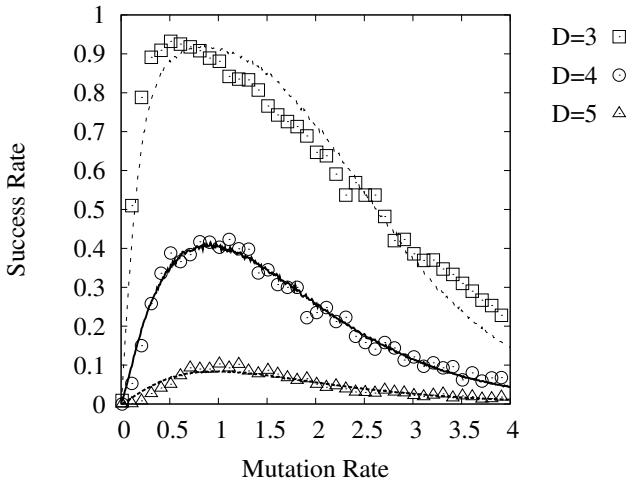

FIG. 3: Success rate curves for $L = 30$, $\gamma = \infty$, $T = 20$, $d_0 = 10$ for different values of the target distance D. The data points are success rates from simulation and the solid curves are fits of Eq. 14 to each set of data.

coverage of epitope space by antibody repertoirs[33, 34]. The essential picture is the following. We begin at an initial distance from the optimal sequence and seek to end up within a certain radius of that optimal sequence. If the mutation rate is large, we explore a larger space in total. However, the volume of the space is larger and the number of points we can try is smaller (because the final population decreases monotonically with the mutation rate), and so the density of coverage of our search space is smaller as well. If our mutation rate is too small, however, we never search far enough to find the target region of sequence space. Fig. 4 is a schematic depiction of this situation, where the shading indicates the density of coverage of each search region.

Let us consider the case of a search that saturates a distance r in the sequence space so that each sequence within that distance of the origin is equally likely to be generated. For sequences of total length L sites that can take on $q = 4$ values, the number of sequences in the space is the volume of the q-ary Hamming ball of radius r in dimension L.

$$V_q(r) = \sum_{i=0}^{r} \binom{L}{i} (q-1)^i. \tag{12}$$

A real evolutionary search of this space does not have a sharp cutoff at r mutations. Rather, the probability of finding a sequence at more than r mutations away falls off monotonically. If we consider the limit in which the saturated search volume completely encompasses the target, then the probability of a random sequence generated within the search volume also being within the target volume is proportional to $V^{-1} = f(r)V_q(r)^{-1}$, where $f(r)$ encodes the overlap between the expanding search volume and the target region. Let us consider the asymptotic behavior of $f(r)$ as $r \to 0$. When $r = 0$, there should be no overlap (unless the initial sequence

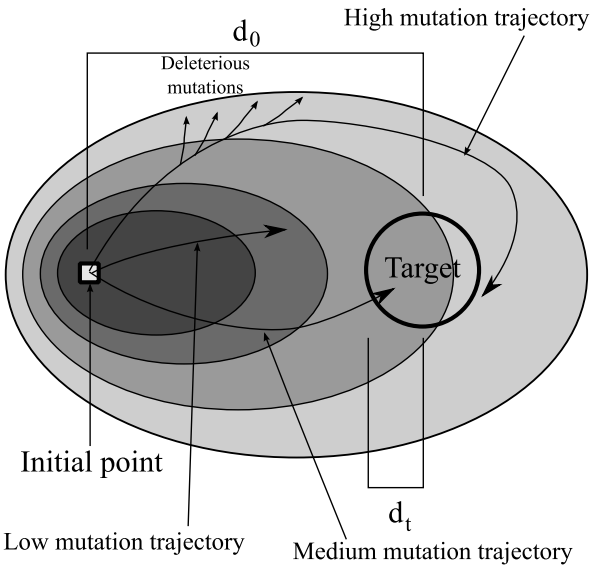

FIG. 4: Schematic diagram of the evolutionary search of sequence space. The ellipses are shaded by density and represent the search region of increasing mutation rate searches of fixed duration. The paths correspond to potential evolutionary trajectories for three mutation rates. One path stops short of the target region, while another wanders around the space in larger steps and so overshoots the target. The branches from the high mutation rate path indicate deleterious mutations that lead to non-replicating sub-populations.

is actually inside the target zone, in which case the success rate will simply be 1), such that if we expand $f(r)$ around $r = 0$ the lowest order behavior we expect to see is $f(r) = \alpha r + O(r^2)$. The parameter α should depend strongly on both the volume of the target region and the distance from the initial sequence to the target region.

Neglecting reversion, the number of different sequences explored by a population of final size P is mP. Taking mP as the number of attempts to hit the target, the success rate is

$$S = 1 - [1 - \alpha r V_q(r)^{-1}]^{mP_f(m)} \tag{13}$$

where $P_f(m)$ is the final population of the system at time T.

To see how S depends on the mutation rate, m, we must relate r to m and the total time, T. Dimensionally, m has units of L/T, so we expect that the distance r scales as $r = \beta m T$, where β is an undetermined constant of proportionality. This corresponds to a directed search, consistent with the strong selection limit in which B-cell evolution operates (for contrast, a random walk would instead scale as $r \approx \sqrt{T}$). Substituting for r in Eq. 13 and defining $a \equiv \alpha\beta T$ and $b \equiv \beta T$,

$$S(m) = 1 - [1 - amV_q(bm)^{-1}]^{mP_f(m)}. \tag{14}$$

This approach has the problem that because m can vary continuously, $r = bm$ need not be an integer. However, the volume of the q-ary Hamming ball is only defined for integer values of the radius. We have made an implicit approximation by replacing a sum over a distribution of mutational radii with the average value. To evaluate this expression for non-integer values of the average saturation distance r we must make some sort of continuous approximation of the function V_q. To do this we first evaluate this function numerically and then construct a 5th order polynomial fit. This continuously interpolates values of V_q without introducing maxima or minima to the function.

We now treat a and b as fitting parameters to compare this predicted form with the success rate curves we measured previously. We compare our predicted functional form, Eq. 14, with the data (Fig. 3), using the measured number of unique sequences from the simulation. The predicted curves fail in cases where the success rate is very large at low mutation rates and in cases where the success rate is very small all around. Despite the fact that the theory effectively assumes that the search space is searched evenly, without a driven component that one would expect from the infinite selection limit, the curves fit very well to the simulations for a range of parameter values. This suggests that the effect of selection in fast macroevolution is to narrow the volume of the search space quantitatively, rather than to change the fundamental dynamics (and thus the scaling with T) of the search. Put another way, it would appear that the role of selection in the immune system is mainly to amplify beneficial discoveries found following the initial random exploration, as opposed to guiding the search step by step. This result contrasts with the long-time case, in which selection dominates the dynamics.

By studying the scaling of a and b, we can understand whether the search process is ballistic (as our simple dimensional analysis predicted), diffusive, or a complex mixture of behaviors. We expect the fitting parameters a and b to scale linearly with time. Moreover, a should change with the target radius, but b should not because the factors contributing to it depend only on the dynamics of the search, not its conclusion. Because the parameter a comes from the leading expansion of $f(r)$, it in particular tells us about the development of the overlap of the leading edge of the search volume to the target area. The parameter b on the other hand comes from the volume of the search space and so tells us how the search volume expands with distance.

We have extracted these fitting parameters from a number of success rate curves ($d_0 = 4, D = 2$; $d_0 = 6, D = 3$; $d_0 = 9, D = 4$) chosen to have the largest dynamic range across the range of durations $5 \leq T \leq 25$. The parameter b increases approximately linearly with T as expected: straight line fits to the data on the log-log plot yield an exponent of 0.910 ± 0.02 over the observed range (Fig. 5). On the other hand, the parameter a changes with time much faster than anticipated (the best-fit power-law exponent is 5.48 ± 0.03). The differ-

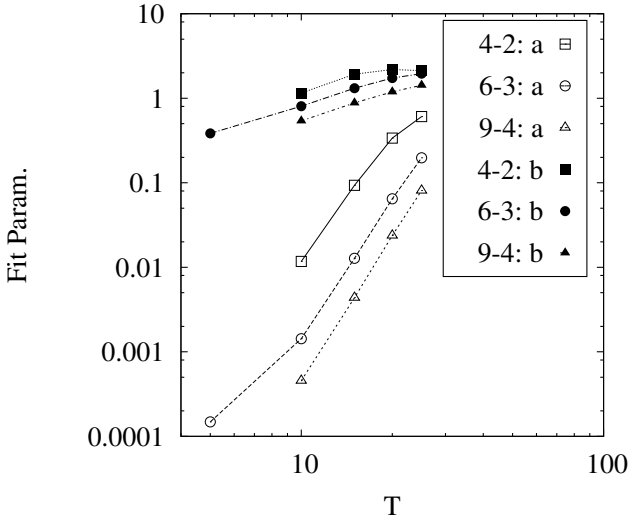

FIG. 5: Fit parameters of Eq. 14 for success curves at times between $T = 3$ and $T = 25$ for $L = 30$ and initial distance/target distance pair $6, 3$, which exhibits the largest dynamic range of success rates in our data set. The success curves for these points were evaluated with 2.5×10^6 trials. The parameter b depends almost linearly on time for central values from $T = 5$ to $T = 20$ ($b\, T^{0.91\pm0.02}$) but deflects at the edges. The parameter a however changes very sharply with time in contrast to the prediction of the leading-order effect.

ence in the time scaling between a and b suggests that the shape of the leading edge of the search volume is changing with time. In essence, the $f(r)$ we proposed above is actually $f(r, T)$, and a more detailed theory that captures the evolution of the leading edge is necessary to understand the a scaling. Overall, though, the theory fits the simulation data remarkably well, which suggests that the volumetric picture captures the main features of the dynamics.

D. Optimal Mutation Rate

Let us consider the mutation rate which maximizes the rate of success over many trials for a specific problem. This mutation rate, corresponding to the peak of the success rate curve, is the optimal mutation rate for that problem. From the simulations, we can compute the optimal mutation rate given the time T, initial distance d_0 (corresponding to the maximum number of beneficial mutations that can be achieved), and target number of beneficial mutations D. We determine this optimal mutation rate empirically by trying mutation rates from 10^{-2} per generation up to 4 per generation, in increments of 10^{-2}. We restrict ourselves to $d_0 < L/2$, as otherwise we are in a regime where an arbitrary random string is closer to the epitope than our initial guess.

Because the dynamics of our system are dominated by the discovery of a successful sequence rather than the maintenance of a population of that sequence, the error

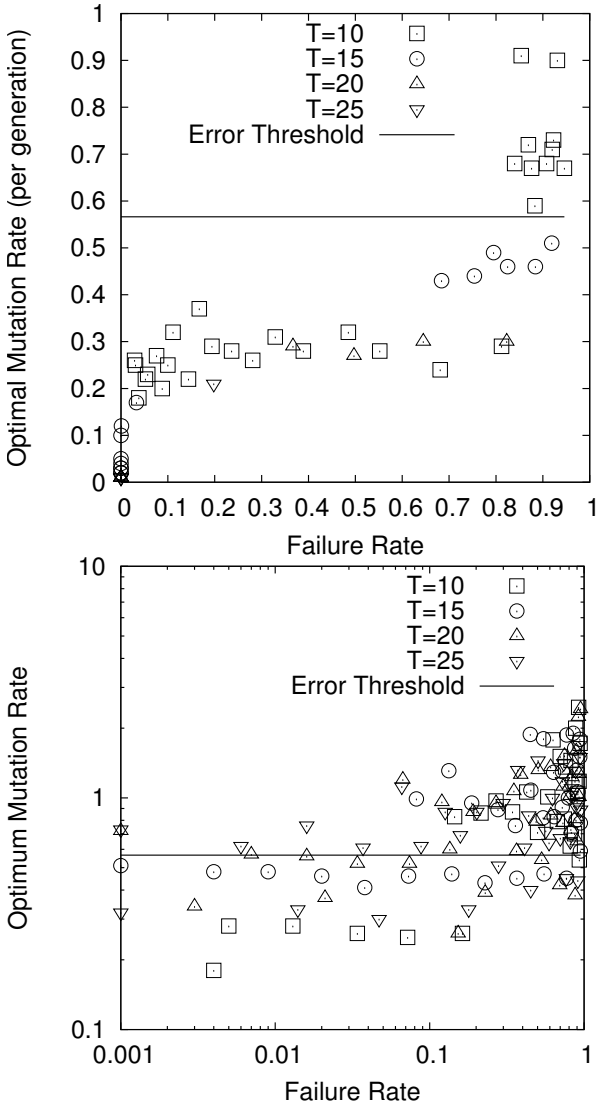

FIG. 6: Optimal mutation rate versus the failure rate for $L = 150$ (top) and $L = 30$ (bottom) for times $T = 10, 15, 20,$ and25 and for various values of $d_0 = [1, 17]$ and the success threshold $D = [1, d_0 - 1]$. The horizontal line indicates the error threshold for this system. For high failure rates, the optimal mutation rate is above the error threshold.

threshold does not necessarily limit the optimal mutation rate during the initial discovery phase. This is in contrast to the usual case, in which populations with mutation rate above the error threshold are unstable, regardless of their fitness. The idea is that the system follows the brief period of mutation above the error threshold with a period of low mutation during which those sequences that were discovered may be amplified without being lost. We do in fact find parameter ranges in which our system prefers to be above the error threshold. When the success rate is large and D is small compared to d_0, then the optimal mutation rate lies below the error threshold, from 0.3 to 0.6 per generation (and so in some cases may in fact be smaller than that of the real immune sys-

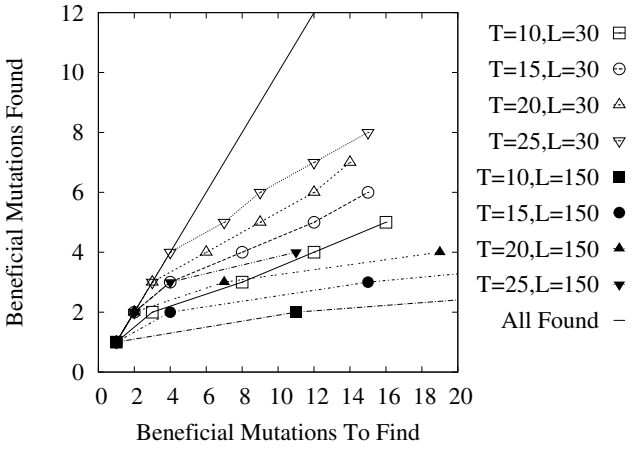

FIG. 7: Number of beneficial mutations found by the adaptive immune system as a function of the total number of possible beneficial mutations for a sequence of length $L = 30$ (hollow symbols) and $L = 150$ (filled symbols). For these curves we fix the mutation rate per generation to be 0.5, which is consistent with biological values for the hypermutation rate in B-cells. The immune system finds the optimum up to a point, beyond which it cannot keep up with the potential number of beneficial mutations. As the immune response duration is lengthened, this point encompasses an increasing number of mutations. The solid line corresponds to all possible mutations being found.

tem dynamics). However, as the success rate drops then the optimal mutation rate rises above the error threshold (Fig. 6). Random guesses can sometimes find the target sequence, even if they hurt the total growth rate of the B cell population. This suggests that the immune system is generally operating in the reliable regime, rather than trying to bridge large evolutionary distances during the period of adaptation.

The hypermutation rate of the immune system was recently studied theoretically [35], and despite the very different perspective from which that study starts, it predicts an optimal rate of about 50% of offspring cells having a single mutation. Despite different assumptions, our model reproduces mutation rates consistent with this optimum over parameter ranges in which we expect the effect of short-time constraints on the evolutionary dynamics should be small. This is consistent with the idea that the optimal mutation rate is normally limited by the error threshold [17, 18].

If the immune system is operating near optimal, then the number of beneficial mutations that are likely to accumulate in this case tells us how far afield memory B cells are likely to be from their initial naive progenitors. This in turn tells us the degree of adaptation that can be expected via hypermutation, and determines how many mutations the immune system must be able to sustain. This tells us that the spacing between features of the sequence space is at least that large. We plot the results in Fig. 7 for the two sequence lengths that we consider. If sufficient time is available, the immune system is able to find all of the potential beneficial mutations that are available. However, as the number of potential beneficial mutations increases, the immune system only finds a decreasing portion. The number of beneficial mutations at which this turning point occurs scales linearly with the duration of the primary immune response. In the case of an immune response of relatively long duration ($T = 25$), the discovery of up to four or five beneficial point mutations seems possible. In the case of the longer sequence ($L = 150$), very little progress is made beyond a single beneficial mutation. However even in the most stringent case of $T = 10$, $L = 150$, at least one beneficial mutation can be found 18% of the time for a single epitope. Even a single point mutation has been found to be responsible for large changes in affinity [36].

III. DISCUSSION

Here, we investigated the dynamics of a short-time evolutionary search for a system-wide goal. In the model, the rate of phenotypic exploration is fast enough that old populations do not become extinct before new beneficial mutations are discovered. As such, the system remembers the evolutionary trajectory that led to the final state, leading to a logarithmic correction to the population count. This particular aspect is a direct consequence of the short time scales involved in the evolutionary dynamics rather than of interference between fixation and mutation. The other factor is the collective success or failure of the search. As such, one expects the parameters of the evolutionary dynamics to be optimal from a system point of view rather than an individual point of view. In cases where the success rate is low, this leads to a relaxation of the error threshold constraint on the optimal mutation rate. However, for the majority of parameter values, the error threshold still bounds the optimal mutation rate.

The mutation rate only exceeds the error threshold when the problem is difficult (the overall success rate is small). In these cases, the optimal strategy is to generate large numbers of highly distributed sequences in hope of finding the target region, at which point the system can make a more directed search. It does not appear that the immune system is generally operating in this regime, as evidenced by observations of a hypermutation rate of 0.5 per generation averaged over the immune response [32]. However, it has been shown that a phasic schedule of mutation, with periods of high mutation punctuating intervals of mutation-free growth, is likely to provide a strong benefit relative to a constant mutation rate [19, 37]. A phasic schedule is expected to be especially advantageous as the amount of time available increases, as repeated random search combined with strong selection pressure and low mutation rate of the positively selected cells will outperform the evolutionary dynamics that result from simply having a high mutation rate.

If the immune system is utilizing intervals of high mu-

tation beyond the error threshold, it has implications for the coevolution of an invading virus and the adaptive immune system. This situation has been studied in [24], in which the error catastrophes for the virus and the immune response place bounds on the mutation rates of both systems. Over the short time, the immune system may be able to outrace the initial adaptation of a virus by having an anomalously high mutation rate. However, if the initial attempt failed, one would expect that a system with a high mutation rate becomes unstable and is unable to maintain pressure on the evolving virus. As such, the short timescale over which the adaptive immune response occurs may introduce an additional regime of behavior in the response to a highly adapting virus, if the immune system is able to quickly defeat the virus by outpacing it on the time scale on which the error threshold is less relevant.

Another point of interest in earlier theoretical studies has been the structure of the epitope/antibody affinity space. Cohn and Langman [38] used an argument about the total number of B cells in small organisms to propose the minimum necessary repertoire of naive B cells needed to respond to any plausible invader. If one considers the consequences of an adaptive response operating in the space of possible specificities, the need to densely cover all possible epitopes is strongly reduced. Instead, the blood need only contain naive B cells that are close enough to each epitope that they can evolve to affinity mature. To understand just how diverse the naive repertoire can be, we compute the number of beneficial mutations generated in our model and find it to be four or five. This number sets the necessary scale of coverage of the initial sequence space as well as the minimal size of the buffer around self epitope reactivity. Knowledge of the structure of the epitope/antibody affinity space is important for developing a conceptual framework for understanding autoimmune disorders produced by age, such as rheumatoid arthritis [39, 40], and those produced by mis-adaptation to an invader [41, 42]. The structure of this space also influences viral escape [43] and viral evolution.

Our finding that the optimal mutation rate can exceed the error threshold has implications for the design of computational optimization strategies. In difficult problems, it can be better to make large random jumps in the the search space in combination with local refinement rather than to make a simple directed search. This is analogous to the phasic schedule of mutation [37] discussed above. It is also akin to the well-known fact that it is more efficient to search a high-dimensional space by drawing points at random rather than from a grid with uniform spacing—this is the basis of the Monte Carlo method [44].

To apply our results to algorithmic design, it will be important to account for the fact that such algorithms typically use a fixed population rather than one that grows or shrinks. Death and birth rates are thus less relevant than comparisons of the fitness of different members of the population. For example, in such a system, if one wished to search the space in a trans-error threshold manner it would be possible to specify that new states of lower fitness than their progenitor are not added to the population pool. This would remove much of the stability issue with trans-error threshold mutation and might push the optimal mutation rate even higher (though in this case, optimal must be measured with respect to computational time required for solution rather than generations). It would be interesting to derive general rules for identifying the optimal strategy in evolutionary dynamics with constraints, like the short-time limit discussed here.

IV. ACKNOWLEDGMENTS

We would like to thank Martin Weigert and Haochu Huang for helpful discussions. S.M.A.T. was funded by the International Human Frontier Science Program Organization (HFSP). N.G. was supported by a Kadanoff-Rice Fellowship (NSF DMR-MRSEC 0820054) and BSD RAC seed funds from the University of Chicago.

[1] C. Wilke, BMC evolutionary biology **5**, 44 (2005), ISSN 1471-2148.
[2] D. Saakian, E. Munoz, C. Hu, and M. Deem, Physical Review E **73**, 041913 (2006).
[3] J. Park and M. Deem, Physical review letters **98**, 58101 (2007).
[4] J. Sun and M. Deem, Physical review letters **99**, 228107 (2007).
[5] A. Peters and U. Storb, Immunity **4**, 57 (1996).
[6] V. Odegard and D. Schatz, Nature Reviews Immunology **6**, 573 (2006).
[7] L. Bogarad and M. Deem, Proceedings of the National Academy of Sciences **96**, 2591 (1999).
[8] A. Oyama, S. Obayashi, and T. Nakamura, Applied Soft Computing **1**, 179 (2001).
[9] S. Woon, O. Querin, and G. Steven, Structural and Multidisciplinary Optimization **22**, 57 (2001).
[10] P. Hajela and E. Lee, International journal of solids and structures **32**, 3341 (1995).
[11] D. Wilson et al., Proceedings of the National Academy of Sciences USA **72**, 143 (1975).
[12] S. Kleinstein and J. Singh, Journal of Theoretical Biology **211**, 253 (2001).
[13] S. Kleinstein and J. Singh, International Immunology **15**, 871 (2003).
[14] F. Celada and P. Seiden, European Journal of Immunology **26**, 1350 (1996).
[15] M. Deem and H. Lee, Physical Review Letters **91**, 68101 (2003).
[16] J. Sun, D. Earl, and M. Deem, Modern Physics Letters

B **20**, 63 (2006).
[17] M. Eigen, Naturwissenschaften **58**, 465 (1971).
[18] M. Eigen, J. McCaskill, and P. Schuster, The Journal of Physical Chemistry **92**, 6881 (1988).
[19] C. Wylie, A. Trout, D. Kessler, and H. Levine, PLoS Genetics **6**, e1001108 (2010).
[20] J. Farmer, N. Packard, and A. Perelson, Physica D: Nonlinear Phenomena **22**, 187 (1986).
[21] G. Woodcock and P. Higgs, Journal of theoretical biology **179**, 61 (1996).
[22] N. Takeuchi and P. Hogeweg, BMC evolutionary biology **7**, 15 (2007).
[23] M. Shlomchik, S. Litwin, and M. Weigert, Prog. Immunol **7**, 415 (1989).
[24] C. Kamp and S. Bornholdt, Physical Review Letters **88**, 68104 (2002).
[25] N. Michael, T. Martin, D. Nicolae, N. Kim, K. Padjen, P. Zhan, H. Nguyen, C. Pinkert, and U. Storb, Immunity **16**, 123 (2002).
[26] C. Wang, R. Harper, and M. Wabl, Proc. Natl. Acad. Sci **101**, 7352 (2004).
[27] J. Uhr, M. Finkelstein, and J. Baumann, Journal of Experimental Medicine **115**, 655 (1962).
[28] P. Hodgkin, J. Lee, and A. Lyons, Journal of Experimental Medicine **184**, 277 (1996).
[29] M. Davenport, C. Fazou, A. McMichael, and M. Callan, The Journal of Immunology **168**, 3309 (2002).
[30] E. Hawkins, J. Markham, L. McGuinness, and P. Hodgkin, Proceedings of the National Academy of Sciences **106**, 13457 (2009).
[31] M. Radmacher, G. Kelsoe, and T. Kepler, Immunology and cell biology **76**, 373 (1998).
[32] M. Weigert, Proc. Natl. Acad. Sci. USA **81**, 3180 (1984).
[33] G. Weisbuch, Journal of theoretical biology **143**, 507 (1990).
[34] R. Hightower, S. Forrest, and A. Perelson, in *Proceedings of the 6th International Conference on Genetic Algorithms* (Citeseer, 1995), pp. 344–350.
[35] J. Zhang and E. Shakhnovich, PLoS Comput Biol **6**, e1000800 (2010).
[36] U. Weiss and K. Rajewsky, Journal of Experimental Medicine **172**, 1681 (1990).
[37] T. Kepler and A. Perelson, Proc. Natl. Acad. Sci. USA **92**, 8219 (1995).
[38] M. Cohn and R. Langman, Immunological Reviews **115**, 11 (1990).
[39] D. Trentham, A. Townes, and A. Kang, Journal of Experimental Medicine **146**, 857 (1977).
[40] J. Edwards and G. Cambridge, Nature Reviews Immunology **6**, 394 (2006).
[41] A. Davidson and B. Diamond, New England Journal of Medicine **345**, 340 (2001).
[42] C. Benoist and D. Mathis, Nature Immunology **2**, 797 (2001).
[43] N. Izmailian, V. Papoyan, V. Priezzhev, and C. Hu, Physical Review E **75**, 41104 (2007).
[44] M. P. Allen and D. J. Tildesley, *Computer Simulation of Liquids* (Oxford University Press, New York, 1987).